AGU ADVANCING EARTH AND SPACE SCIENCE

Geophysical Research Letters®

RESEARCH LETTER
10.1029/2021GL094780

Key Points:

- The decline of Arctic sea ice volume has slowed down in recent years under increasingly warm atmospheric and oceanic conditions
- The slowdown is due to weak ice export and strong ice growth which serve as a negative feedback to retard the ice volume decline
- Increases in dynamic open water creation because of an accelerating thin ice cover play a role in stimulating ice growth in recent years

Correspondence to:
J. Zhang,
zhang@apl.washington.edu

Citation:
Zhang, J. (2021). Recent slowdown in the decline of Arctic sea ice volume under increasingly warm atmospheric and oceanic conditions. *Geophysical Research Letters*, *48*, e2021GL094780. https://doi.org/10.1029/2021GL094780

Received 9 JUN 2021
Accepted 20 AUG 2021

Recent Slowdown in the Decline of Arctic Sea Ice Volume Under Increasingly Warm Atmospheric and Oceanic Conditions

Jinlun Zhang[1]

[1]Polar Science Center, Applied Physics Laboratory, University of Washington, Seattle, WA, USA

Abstract A model study shows that the decline of Arctic sea ice volume (SIV) slows down during 2007–2020 with increasingly warm atmospheric and oceanic conditions. The slowdown of the SIV decline is because the decrease in ice export from the Arctic exceeds the decrease in net ice production within the Arctic. The relatively strong decrease in ice export occurs when the increase in ice motion is lower than the decrease in SIV. The relatively weak decrease in net ice production is due to strong increases in ice growth as thinner ice grows faster than thicker ice under freezing conditions. The ice growth increases are closely correlated with and benefit from increases in open water creation caused by enhanced ice divergence and shear as thinner ice is easier to deform.

Plain Language Summary Results from the Pan-arctic Ice-Ocean Modeling and Assimilation System (PIOMAS) show significant decline of Arctic sea ice volume (SIV) in the past decades. However, the SIV decline is slowing down during 2007–2020 with increasingly higher air and ocean temperatures, which is in line with satellite CryoSat-2 observations of largely stabilized SIV since 2011. The slowdown of the SIV decline is because of relatively strong decreases in ice export from the Arctic and increases in ice growth in the Arctic. The relatively strong increase in ice growth in 2007–2020 is because thinner and less compact ice, which is the norm in recent years, has much higher growth rates than thicker ice under freezing conditions. Thinner ice also moves faster and deforms more, which tends to create more open water to stimulate ice growth in 2007–2020. Thus, the ice export and growth processes play a role in slowing down the SIV decline in recent years and may continue to play that role in the future.

1. Introduction

Significant decline of Arctic sea ice has been observed in the past decades (e.g., IPCC Special Report on Ocean and Cryosphere, 2019). The decline occurred after years of decreases in sea ice volume (SIV) or thickness (e.g., Kwok & Rothrock, 2009; Lindsay & Schweiger, 2015), in conjunction with increasing surface air temperature (SAT) (Richter-Menge et al., 2016; Serreze et al., 2007). Satellite observations reveal a drastic retreat of Arctic sea ice in summer 2007, with a record low summer ice extent (Stroeve et al., 2008; Zhang et al., 2008). Since then, summer Arctic sea ice extent has been at the lowest levels and the 2007 record low summer ice extent was broken in 2012 (e.g., Parkinson & Comiso, 2013). However, no new record low summer ice extent has been observed since 2012 (e.g., Francis & Wu, 2020). In addition, the CryoSat-2 (CS2) derived SIV in the Arctic Ocean, defined here as the combined Arctic Basin and Chukchi, Beaufort, East Siberian, Laptev, Kara, and Barents marginal seas, has shown no clear trends since 2010 (Figure 1; also see Li et al., 2020).

The lack of decrease in the CS2 observed Arctic SIV in 2010–2020 is in glaring contrast to much of the past decades when Arctic SIV or thickness decreased steadily. While the lack of a new record low in summer ice extent since 2012 may be attributed to an abrupt atmospheric shift during August/early September (Francis & Wu, 2020), it is not yet clear why Arctic SIV is more or less stabilized in recent years. One cannot help but ask: Is the lack of CS2 SIV trends since 2010, together with the lack of new record low summer ice extent since 2012, an indication of a slowdown in the decline of Arctic sea ice in recent years? If so, what caused the slowdown? This study aims to shed some light on these questions by examining the changes in Arctic SIV and associated dynamic thermodynamic sea ice processes over the period 1979–2020. We conducted a model hindcast using the coupled Pan-arctic Ice-Ocean Modeling and Assimilation System (PIOMAS,

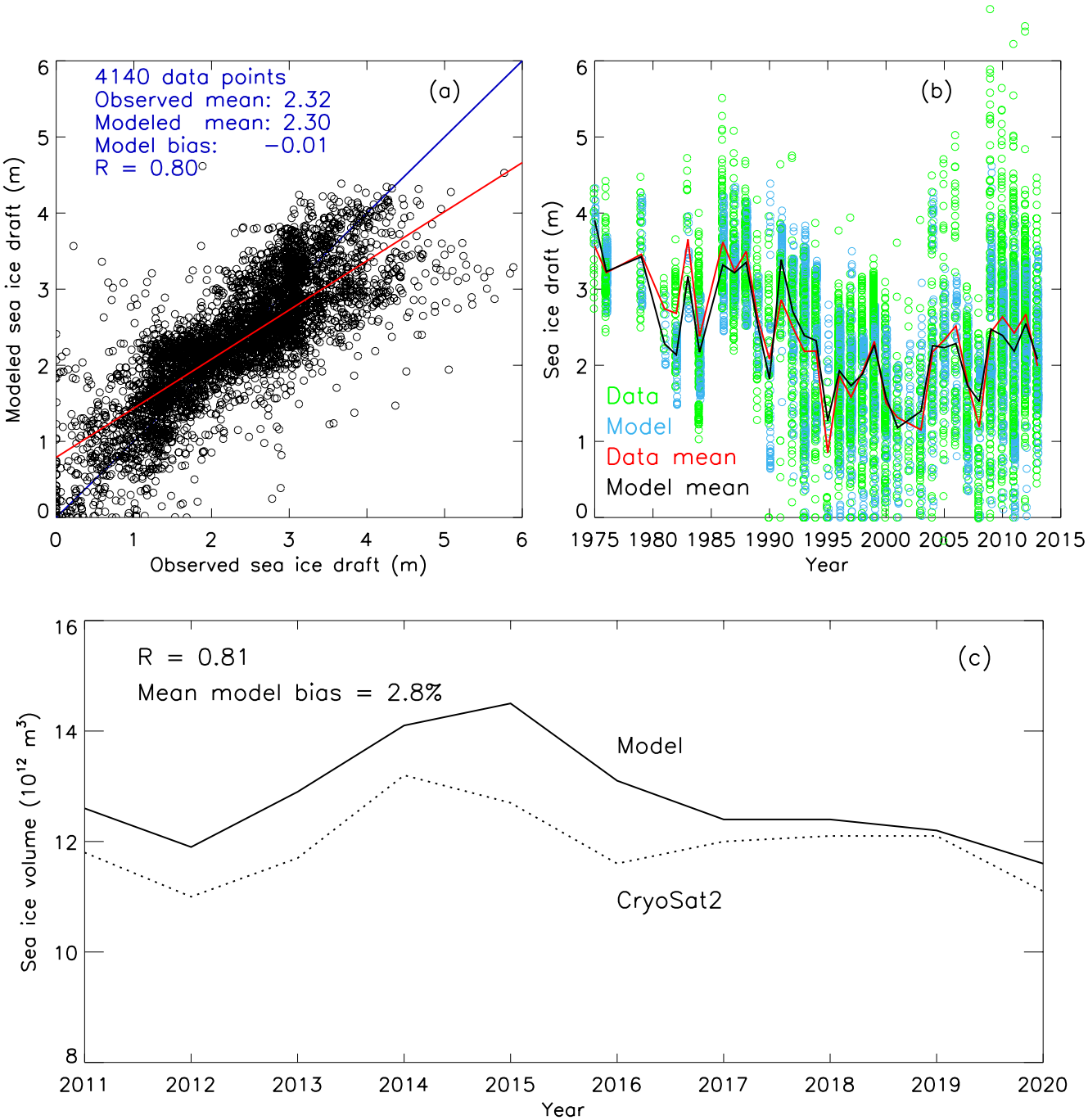

Figure 1. (a) Model simulated sea ice draft compared with all corresponding sea ice draft (or thickness converted to draft) observations in space and time over the period of 1975–2013 available from the Sea Ice Climate Data Record (CDR, http://psc.apl.washington.edu/sea_ice_cdr/; R. Lindsay, 2013; R. W. Lindsay, 2010). The observations include those from submarine-based upward looking sonars (ULS) over much of the central Arctic Basin (Rothrock et al., 2008), from moored ULS in the Chukchi and eastern Beaufort seas (Melling & Riedel, 2008), in the central Beaufort Sea (The Beaufort Gyre Exploration Project, Krishfield et al., 2014), and in Fram Strait area (Witte & Fahrbach, 2005), from airborne electromagnetic induction instruments (Haas et al., 2009), and from the airborne laser altimeters of the NASA Operation IceBridge Project (Kurtz et al., 2013). The IceBridge data are sea ice thickness data, which are converted into draft data by simply dividing by 1.12. The electromagnetic data are combined ice and snow thickness data, which are converted to draft data using modeled snow depth following Rothrock et al. (2008) (also see Zhang et al., 2015). The blue line indicates equality and the red line represents the best fit to the observations. The number of total observation points, model and observation mean values, model bias (mean model-observation difference), and model-observation correlation (R) are listed. (b) Observations and corresponding model results (circles) for those individual years with observations available and annual observation and model means (lines). (c) Model simulated and CS2 estimated mean sea ice volume during January–April and October–December of the year over the Arctic Ocean excluding the pole hole north of 88 N where no CS2 data are available.

Zhang & Rothrock, 2003). By addressing these questions, we hope this model study will help to assist the design of observational studies to further improve our understanding of the variability and trends of the Arctic sea ice cover.

2. Model Description

PIOMAS consists of the thickness and enthalpy distribution (TED) sea ice model (Zhang & Rothrock, 2003) coupled with the POP (Parallel Ocean Program) ocean model (Smith et al., 1992). The TED sea ice model simulates the evolution of a 12-category ice thickness distribution and ice ridging processes explicitly following Hibler (1980). Ice motion is solved following Zhang and Hibler (1997) based on a momentum equation that consists of a teardrop plastic rheology describing a relationship among ice internal stress, strain rate, and mechanical strength (Zhang & Rothrock, 2005). The ice model also includes 12-category snow depth described by a snow distribution conservation equation (Flato & Hibler, 1995). More model information can be found in Schweiger et al. (2011). The model is driven by daily NCEP/NCAR reanalysis atmospheric forcing including 10-m surface winds and 2-m SAT (Zhang & Rothrock, 2003). Model spin-up consists of an integration of 30 years using 1948 reanalysis forcing repeatedly, initialized with a constant 2 m sea ice thickness in the areas of SAT at or below 0°C, ocean temperature and salinity climatology (Levitus, 1982), and zero ice and ocean velocity. After this spin-up the model proceeds to simulate the period 1948–2020 without data assimilation. Model results over 1979–2020 are examined here. We focus on the period 2007–2020 because of the possible slowdown of the decline in Arctic SIV. Results from the period 2007–2020 are compared with those from the period 1979–2006.

3. Results

To examine model behavior in simulating SIV, modeled sea ice draft (or ice thickness converted to ice draft) is compared with various sources of sea ice draft/thickness observations collected over the period of 1975–2013, available from the Sea Ice Climate Data Record (CDR, R. Lindsay, 2013; R. W. Lindsay, 2010) (Figure 1). Overall, the model compares well with the available observations (4,140 data points in total) over the period 1975–2013 with a near-zero mean bias and high correlation ($R = 0.80$), although some individual points may show model-observation differences of up to several meters (Figure 1a). The model overestimates thin ice and underestimates thick ice. It captures most of the ups and downs of the spatiotemporally averaged values of sparsely distributed ice draft observations on an annual time scale (Figure 1b). The general agreement suggests that the model can reproduce the observed interannual variability reasonably well over 1975–2013. The model also compares well with the CS2 derived Arctic SIV, averaged over January–April and October–December, during the period 2010–2020, with mean model bias of 2.8% and correlation of $R = 0.81$. As mentioned before, CS2 does not show clear SIV trends since 2010, and neither does the model.

The model simulates a significant decline in Arctic SIV since 1987 (Figure 2a). The simulated sea ice area is in reasonable agreement with satellite observations, with mean model bias of 5.4% and model-observation correlation of $R = 0.96$ (Figure 2b). The SIV decline is closely correlated with increasing reanalysis SAT ($R = -0.90$) and model upper (60 m) ocean temperature (UOT) ($R = -0.86$) (Figures 2a and 2c). On average, SIV is 20.5×10^{12} m^3 over 1979–2006 and 13.4×10^{12} m^3 over 2007–2020, a decrease of 34.6% in the later period (Table 1). During 2007–2020, SIV decreases strongly in all seasons (Figure 3a), which corresponds to increases in SAT in fall (October–December), winter (January–March), and early spring (April–June) (Figure 3b) and increases in UOT in summer (July–September) and part of fall (Figure 3c). The decreasing rate in SIV is -0.29×10^{12} m^3/year in 1979–2006 and -0.10×10^{12} m^3/year in 2007–2020. Thus, the decreasing rate in the later period is nearly 3 times lower than in the earlier period, indicating a significant slowdown in the decline of SIV in recent years. The simulated slowdown is consistent with the behavior of the CS2-derived SIV, which shows no clear trending over 2010–2020 (Figure 1c), as mentioned before. Meanwhile, the increasing trend of SAT (UOT) over 2007–2020 is found to be 0.129 C/year (0.020 C/year), higher than 0.087 C/year (0.011 C/year) over 1979–2006. This suggests that the recent slowdown in the decline of Arctic SIV occurred under increasingly warm atmospheric and oceanic conditions.

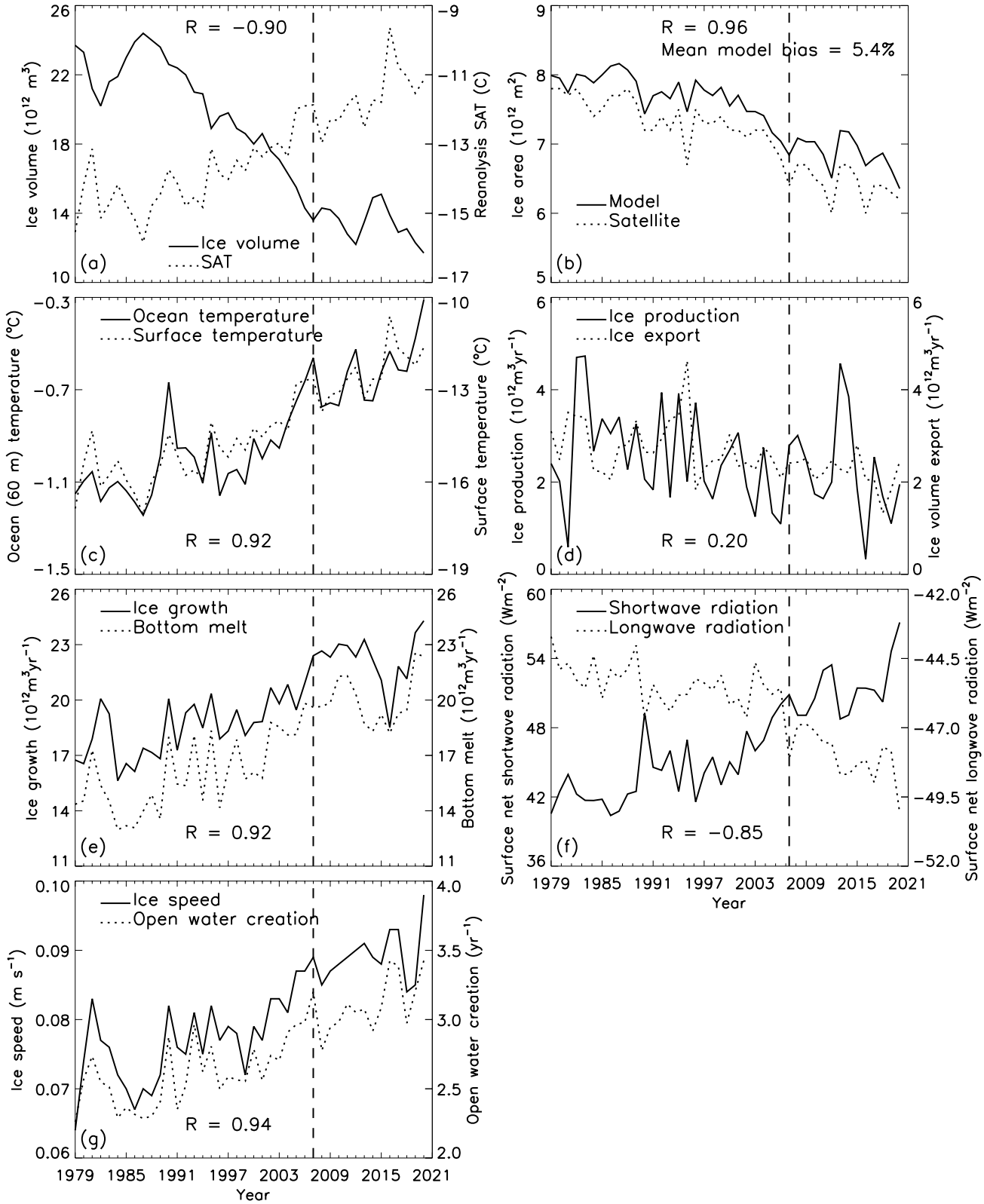
R = −0.90
Ice volume
SAT
(a)
Ice volume (10^{12} m^3)
Reanalysis SAT (C)
R = 0.96
Mean model bias = 5.4%
Model
Satellite
(b)
Ice area (10^{12} m^2)
Ocean temperature
Surface temperature
R = 0.92
(c)
Ocean (60 m) temperature (°C)
Surface temperature (°C)
Ice production
Ice export
R = 0.20
(d)
Ice production ($10^{12}m^3yr^{-1}$)
Ice volume export ($10^{12}m^3yr^{-1}$)
Ice growth
Bottom melt
R = 0.92
(e)
Ice growth ($10^{12}m^3yr^{-1}$)
Bottom melt ($10^{12}m^3yr^{-1}$)
Shortwave rdiation
Longwave radiation
R = −0.85
(f)
Surface net shortwave radiation (Wm^{-2})
Surface net longwave radiation (Wm^{-2})
Ice speed
Open water creation
R = 0.94
(g)
Ice speed (m s^{-1})
Open water creation (yr^{-1})
1979 1985 1991 1997 2003 2009 2015 2021
Year

Figure 2.

Table 1
1979–2006 and 2007–2020 Mean Values and Change in the 2007–2020 Mean Over the 1979–2006 Mean for Some Variables of NCEP/NCAR Reanalysis Data and Model Results Averaged Over the Arctic Ocean

	1979–2006 mean	2007–2020 mean	Change (%)
Reanalysis surface air temperature (C)	−14.0	−11.6	**17.1**
Reanalysis surface wind speed (m s^{-1})	4.78	4.91	**2.7**
Ice volume (10^{12} m^3)	20.5	13.4	**−34.6**
Ocean (60 m) temperature (C)	−1.01	−0.62	**38.6**
Surface temperature (C)	−15.07	−12.44	**17.5**
Ice production (10^{12} m^3 yr^{-1})	2.56	2.25	−13.3
Ice export (10^{12} m^3 yr^{-1})	2.77	2.22	**−19.9**
Ice growth (10^{12} m^3 yr^{-1})	18.52	22.26	**20.2**
Bottom melt (10^{12} m^3 yr^{-1})	15.96	20.01	**25.4**
Surface net shortwave radiation (Wm^{-2})	44.16	51.42	**16.4**
Surface net longwave radiation (Wm^{-2})	−45.40	−48.04	**−5.8**
Dynamic open water creation (yr^{-1})	2.59	3.11	**20.1**
Ice speed (m s^{-1})	0.077	0.089	**15.6**

Note. Boldface numbers exceed the 95% confidence level when tested using the Student's *t*-test method.

The increasingly warm atmosphere could be a consequence of more heat loss from the surface of the thinner, less compact ice cover and the warming upper ocean because of the atmosphere–ice–ocean interactions. Since PIOMAS is an ice–ocean model not coupled to an atmospheric model, the atmosphere–ice–ocean interactions may not be adequately represented. However, some of the effect of the interactions may be captured by the reanalysis atmospheric forcing used to drive PIOMAS.

What caused the slowdown of the SIV decline in 2007–2020 in an increasingly warm Arctic? To explore this question, sea ice processes affecting SIV are examined. A change in SIV (DV) for a given time (here one year) is determined by a balance between the total (net) ice production (P) inside the Arctic Ocean and ice (volume) export (E) at its open boundaries, mainly Fram Strait (Kwok & Rothrock, 1999), such that D$V = P–E$. Both ice production and ice export are subject to considerable interannual variability and have been slightly decreasing over the past decades (Figure 2d). During 2007–2020, ice production increases in winter and fall, but decreases more in spring and summer (Figure 3d). As a result, ice production in 2007–2020 is −13.3% lower than in 1979–2016 (Table 1). Meanwhile, ice export in 2007–2020 decreases in all seasons except summer when the magnitude of ice export is small (Figure 3e), leading to a reduction of −19.9% from the level in 1979–2016 (Table 1).

The decrease in ice production in 2007–2020 is in conjunction with the increases in SAT and UOT in a warming environment. The decrease in ice export is mainly because ice is thinning inside the Arctic Ocean and therefore less available for export (Wang et al., 2021; Zhang et al., 2012), given the small difference (2.7%) in wind speed between these two periods (Table 1). Zhang et al. (2012) also found that when the rate of decrease in SIV or thickness exceeds the rate of increase in ice speed, ice export tends to decrease. Here the simulated SIV decrease in 2007–2020 is −34.6% over the level in 1979–2006, much higher in magnitude than the ice speed increase of 15.6% (Table 1). The large difference in magnitude between the decrease in SIV and the increase in ice speed during 2007–2020 leads to a strong decrease of −19.9% in ice export, higher than the decrease of −13.3% in ice production. Thus, the strong decrease in ice export serves as a negative feedback in response to the decrease in SIV (Zhang et al., 2012).

Figure 2. Annual means over the Arctic Ocean for: (a) ice volume and NCEP/NCAR reanalysis surface air temperature (SAT), (b) model and satellite ice area, (c) ocean temperature in the upper 60 m and temperature on the snow/ice/open-water surface, (d) ice production and ice volume export, (e) ice growth and bottom melt, (f) surface net shortwave and longwave radiation, and (g) ice speed and dynamic open water creation. Correlation (R) between two time series in each panel is indicated. Satellite ice area in (b) is derived using ice concentrations from the Hadley Centre for 1979–2006 and from the National Snow and Ice Data Center (NSIDC) near real time product for 2007 onward.

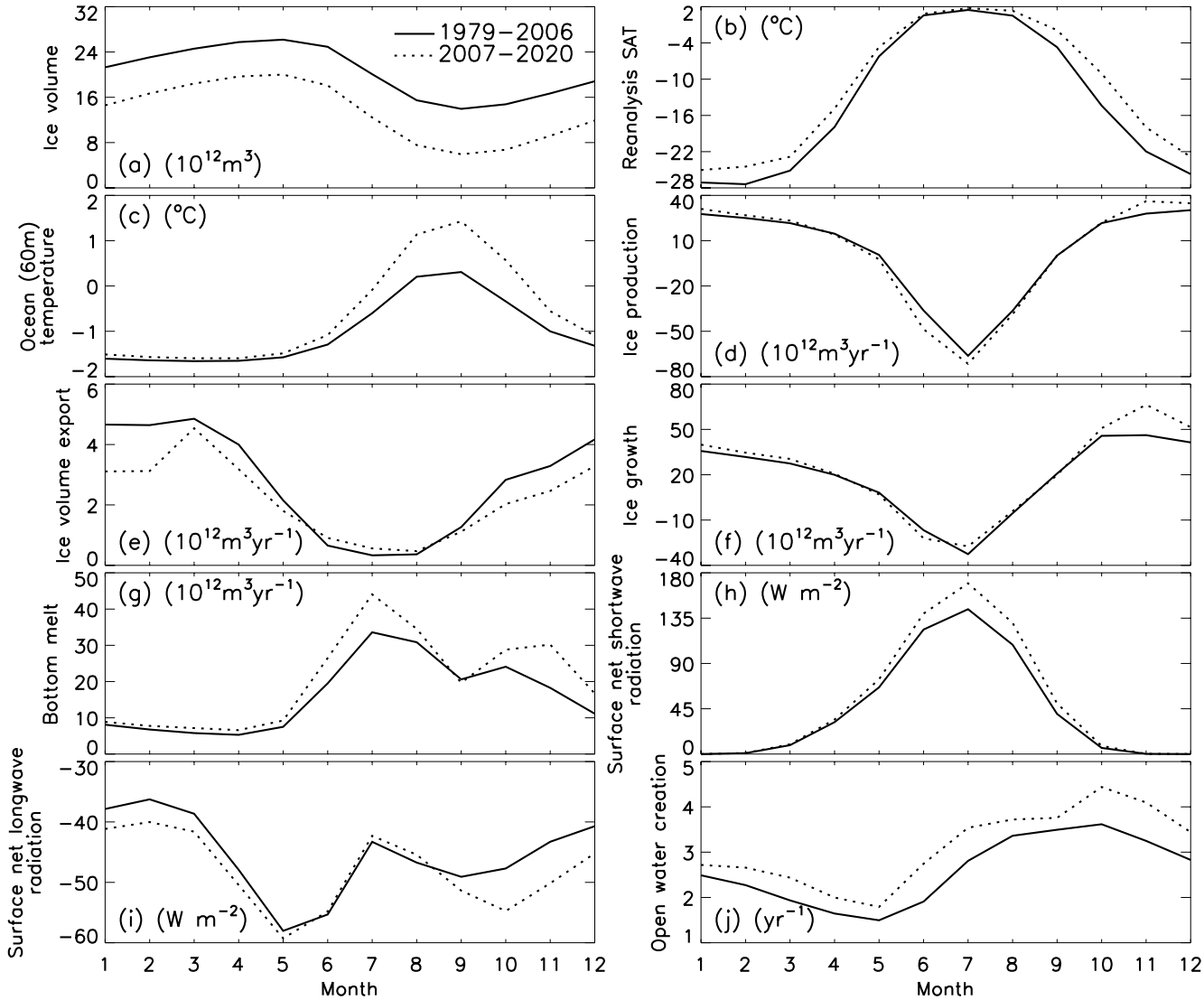

Figure 3. Monthly mean model results and NCEP/NCAR reanalysis surface air temperature (SAT) averaged over the Arctic. The solid line represents the 1979–2006 mean and dotted line the 2007–2020 mean. (a) Ice volume, (b) reanalysis SAT, (c) ocean temperature in the upper 60 m, (d) ice production, (e) ice volume export, (f) ice growth, (g) bottom melt, (h) surface net shortwave radiation, (i) surface net longwave radiation, and (j) dynamic open water creation.

The simulated average ice export is 2.77×10^{12} m^3/year during 1979–2006, higher than the average ice production of 2.56×10^{12} m^3/year (Table 1), leading to a negative D$V = -0.21 \times 10^{12}$ m^3/year. As a result, SIV was declining steadily over that period. During 2007–2020, however, ice export is 2.22×10^{12} m^3/year, lower (though barely) than ice production of 2.25×10^{12} m^3/year (Table 1), leading to a near zero DV. The near zero DV leads to a slowdown in the decline of SIV in 2007–2020, even with increasingly higher SAT and UOT. In other words, a relatively strong decrease in ice export (−19.9%) and a relatively weak decrease in ice production (−13.3%) from the level in 1979–2006 leads to the slowdown of the SIV decline in 2007–2020.

What caused the relatively weak decrease in ice production under the conditions of increasingly higher SAT and UOT in 2007–2020? Here ice production is defined by the difference between ice growth, including both basal growth of sea ice related to conduction of heat through the ice and top surface sea ice melt due to surface atmospheric cooling or heating, and bottom melt, defined here as melt at the bottom and perimeter of ice floes due to ocean heating. Ice growth and bottom melt are controlled by ice thermodynamics calculated following Winton (2000). Both ice growth and bottom melt have been generally increasing in the past decades (Figure 2e, Table 1). Compared to 1979–2006, ice growth in 2007–2020 increases mainly in fall and winter (Figure 3f), while bottom melt increases mainly in late spring and most of summer and fall

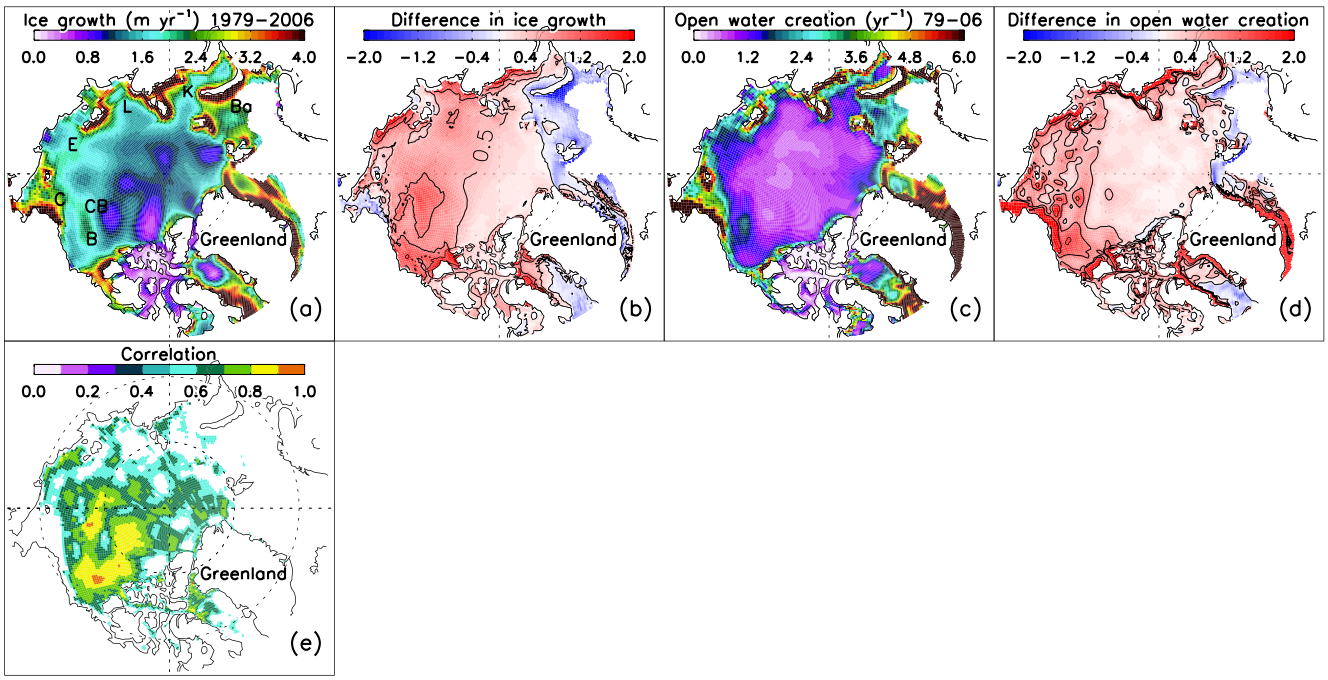

Figure 4. Simulated 1979–2006 mean and the difference between the 2007–2020 mean and the 1979–2006 mean for (a–b) ice growth and dynamic open water creation (c–d). (e) Correlation between ice growth and open water creation over 1979–2020, only correlation values above 0.5 plotted. The Chukchi, Beaufort, East Siberian, Laptev, Kara, and Barents seas and Canada Basin are marked by C, B, E, L, K, Ba, and CB, respectively in (a). Contours are plotted in (b) and (d) for values of 0.0, 0.5, 1.0, and 1.5 m yr^{-1} (b) and yr^{-1} (d).

(Figure 3g). The increase in bottom melt is closely associated with the increase in UOT (Figures 2c and 3c), which is in turn linked to the thinner and less compact ice that allows more absorption of shortwave radiation at the surface in, mainly, late spring and summer (Figures 2f and 3h; Table 1) because of the impact of the ice-albedo feedback (e.g., Holland & Landrum, 2015).

Ice growth is characterized by higher values in the Arctic marginal seas and lower values in the central Arctic (Figure 4a). The increase in ice growth in fall and winter during 2007–2020 occurs in most of the Arctic, especially in the Canada Basin (Figure 4b). The increase is also linked to the thinner and less compact ice in recent years. This is because thin ice and open water have a much higher growth rate than thick ice when they are subject to the same forcing in freezing conditions, as reflected in the strong nonlinear relationship between ice growth rate and ice thickness (Bitz & Roe, 2004; Goosse et al., 2018; Maykut & Untersteiner, 1971). Such a strong nonlinear relationship dictates that ice growth in fall and winter tends to increase in recent years even under increasingly warm atmospheric and oceanic conditions. Note that the increase in winter ice growth differs from Stroeve et al. (2018) that showed decreasing winter ice growth in recent years. However, it agrees with Petty et al. (2018) that showed increasing winter ice growth under warming Arctic conditions. The increase in ice growth in 2007–2020 is also boosted by a reduction in net surface longwave radiation in fall and winter (Figures 2f and 3i; Table 1). The reduction is caused by increasing temperature (Figure 2c) at the snow/ice/open-water surface associated with a thinner, less compact snow-ice cover, which allows for increased upward longwave radiation.

The increase in ice growth is further boosted by an increase in open water creation in 2007–2020, which is higher than in 1979–2006 in all seasons (Figures 2g and 3j, Table 1). Open water creation is a dynamic process induced by ice divergence and shear deformation, which is represented by a term in the sea ice thickness distribution equation (Flato & Hibler, 1995; see Appendix). The increasing dynamic open water creation is highly correlated with increasing ice speed ($R = 0.94$, Figure 2g). This is because a thinner ice cover is more mobile and easier to deform (e.g., Rampal et al., 2009; Spreen et al., 2011; Zhang et al., 2012), leading to higher divergence and shear. The spatial pattern of open water creation resembles that of ice growth, with higher values in the Arctic marginal seas and lower values in the central Arctic (Figure 4c). Also, like the increase in ice growth, the increase in the simulated open water creation occurs in most of

the Arctic, more strongly in most of the Canada Basin (Figure 4d). In fact, the correlation between dynamic open water creation and ice growth is above 0.5 in most of the Arctic and above 0.8 in most of the Canada Basin (Figure 4e) which sees a stronger increase in both ice growth and open water creation in 2007–2020 from the level in 1979–2006. Thus, the increase in open water creation is closely associated with the increase in ice growth, as open water has high ice growth rates in freezing conditions in fall and winter (Maykut & Untersteiner, 1971). In other words, the dynamics-driven increase in open water creation boosts ice growth, which plays a role in the relatively weak decrease in ice production and hence in the slowdown of SIV decline under the conditions of increasingly higher SAT and UOT in the later period.

4. Concluding Remarks

PIOMAS shows a significant decline of Arctic SIV over much of the period 1979–2020, in line with previous studies (e.g., Kwok & Rothrock, 2009; Lindsay & Schweiger, 2015). However, it also shows that the Arctic SIV decline is slowing down during 2007–2020, which is in line with CS2 observations of largely stabilized Arctic SIV over 2011–2020. The slowdown of Arctic SIV decline occurs despite increasingly warm SAT and UOT. The reason for the slowdown of the SIV decline is because of a change in ice mass balance such that the decrease in ice export at the open boundaries of the Arctic exceeds the decrease in net ice production inside the Arctic.

The magnitude of ice export depends on SIV or thickness and ice motion. The relatively strong decrease in ice export in 2007–2020 is attributed mainly to two factors: (a) Ice is thinning inside the Arctic Ocean and therefore less available for export. (b) The increase in ice speed is lower than the decrease in SIV or thickness and unable to drive more ice out of the Arctic (Zhang et al., 2012). Thus, the behavior of ice export at a time of SIV decline serves as a negative feedback to retard the decline.

The relatively weak decrease in net ice production in 2007–2020 is because of a strong increase in ice growth in fall and winter, which compensates for some of the ice loss in summer due to elevated ice melt associated with ice-albedo feedback. The strong increase in ice growth is attributed mainly to three factors: (a) Thinner and less compact ice has much higher growth rates than thicker ice under freezing conditions. (b) There is an increase in dynamic open water creation due to enhanced ice divergence and shear deformation as a thinner ice cover is more mobile and easier to deform. (c) There is a decrease in surface net longwave radiation in fall and winter because of an increase in surface temperature that promotes upward longwave radiation.

Open water creation is closely correlated with ice growth in much of the Arctic, particularly in the Canada Basin where the correlation is often above $R = 0.8$. By increasing the area of open water, the open water creation process helps to boost ice growth in fall and winter in 2007–2020. The behavior in ice growth at a time of SIV decline, aided by increased open water creation induced by increased ice motion and deformation, serves as a negative feedback to retard the decline, and therefore plays a role in the slowdown of the Arctic SIV decline during 2007–2020 under increasingly warm atmospheric and oceanic conditions.

Here, 2007 is selected as a starting year to examine the slowdown of the Arctic SIV in recent years. This is based on the consideration that 2007 saw a record low summer ice extent at that time, before a new record set in 2012. Nevertheless, the selection is somewhat arbitrary, and one can certainly select a different starting year for analysis. However, moderately shifting the starting year away from 2007 (e.g., 2005, 2006, 2008, and 2009) would not fundamentally change this model study's conclusions that a slowdown of the Arctic SIV decline has occurred in recent years.

Note that the model simulated Arctic SIV drops from 1979 to a local minimum in 1982 and then peaks in 1987 (Figure 2a). There is no significant trend in SIV during the period 1979–1987. While there is no significant trend in SIV either during the period 2007–2020, the later period differs from the early period 1979–1987 in two key aspects: (a) SIV in 2007–2020 is much lower than in 1979–1987, and (b) SAT and UOT are climbing increasingly higher in 2007–2020, while dropping in 1979–1987. The thinner ice cover during 2007–2020 leads the ice export and growth processes to play a role in serving as a negative feedback to slow down the SIV decline, which is not seen in 1979–1987. It is expected that such a role may become more prominent in the future. In other words, the slowdown of the Arctic SIV decline may continue for some time in the future unless a stronger Arctic warming than the present would occur. Whether it is true remains to be seen through enhanced observations and modeling.

Appendix: Description of Dynamic Open Water Creation

Dynamic open water creation is caused by ice divergence and shear deformation. It is described in the sea ice thickness distribution equation by a component of the mechanical redistribution function (Flato & Hibler, 1995; also see Hibler, 1980; Thorndike et al., 1975):

$$\psi_0 = \delta(h)\left[\tfrac{1}{2} C_s\left(\Delta - \left|\dot{e}_{kk}\right|\right) + \max\left(\dot{e}_{kk}, 0\right)\right], \tag{A1}$$

where $\delta(h)$ is a delta function, h is ice thickness, C_s is the shear ridging parameter that determines how much of the total mechanical energy dissipation rate is allocated for mechanical redistribution or ridging and is set to 0.5 following the standard case of Flato and Hibler (1995), $\dot{e}_{ij}$ is the ice strain rate tensor, and $\dot{e}_{kk} = \dot{e}_{11} + \dot{e}_{22}$ is the ice divergence rate. In (A1), $\Delta = 4\left[\left(\sigma_I/p + 1/2\right)\dot{e}_I - \left(\sigma_I/p - a\right)\left(1 + \sigma_I/p\right)^{1/2}\dot{e}_{II}\right]$ based on a teardrop plastic rheology (Zhang & Rothrock, 2005), where a is the biaxial tensile stress parameter set to 0.05, $\sigma_I = 1/2\left(\sigma_1 + \sigma_2\right)$, $\dot{e}_I = 1/2\left(\dot{e}_1 + \dot{e}_2\right)$, $\dot{e}_{II} = 1/2\left(\dot{e}_1 - \dot{e}_2\right)$, σ_1 and σ_2 are the principal stresses, and $\dot{e}_1$ and $\dot{e}_2$ are the principal strain rates. The first term in (A1) represents shear induced open water creation, and the second represents divergence induced open water creation (Flato & Hibler, 1995).

Data Availability Statement

PIOMAS output is available at http://psc.apl.uw.edu/research/projects/arctic-sea-ice-volume-anomaly/.

Acknowledgments
This work was funded by the NSF Office of Polar Programs (grants PLR-1603259, PLR-1602985, and NNA-1927785), and the NASA Cryosphere Program (NNX17AD27G). The author thanks A. Schweiger for processing CS2 ice thickness and A.S., H. Stern, and two anonymous reviewers for their constructive comments

References

Bitz, C. M., & Roe, G. H. (2004). A mechanism for the high rate of sea-ice thinning in the Arctic Ocean. *Journal of Climate*, *17*, 3622–3632. https://doi.org/10.1175/1520-0442(2004)017<3623:AMFTHR>2.0.CO;2

Flato, G. M., & Hibler, W. D., III (1995). Ridging and strength in modeling the thickness distribution of Arctic sea ice. *Journal of Geophysical Research*, *100*, 18611–18626. https://doi.org/10.1029/95jc02091

Francis, J. A., & Wu, B. (2020). Why has no new record-minimum Arctic sea-ice extent occurred since September 2012? *Environmental Research Letters*, *15*, 114034. https://doi.org/10.1088/1748-9326/abc047

Goosse, H., Kay, J. E., Armour, K. C., Bodas-Salcedo, A., Chepfer, H., Docquier, D., et al. (2018). Quantifying climate feedbacks in polar regions. *Nature Communications*, *9*(1), 1919. https://doi.org/10.1038/s41467-018-04173-0

Haas, C., Lobach, J., Hendricks, S., Rabenstein, L., & Pfaffling, A. (2009). Helicopter-borne measurements of sea ice thickness, using a small and lightweight, digital EM system. *Journal of Applied Geophysics*, *67*(3), 234–241. https://doi.org/10.1016/j.jappgeo.2008.05.005

Hibler, W. D., III (1980). Modeling a variable thickness sea ice cover. *Monthly Weather Review*, *108*.

Holland, M. M., & Landrum, L. (2015). Factors affecting projected Arctic surface shortwave heating and albedo change in coupled climate models. *Philosophical Transactions of the Royal Society A: Mathematical, Physical & Engineering Sciences*, *373*, 20. https://doi.org/10.1098/rsta.2014.0162

IPCC Special Report on Ocean and Cryosphere. (2019). Retrieved from https://www.ipcc.ch/srocc/

Krishfield, R. A., Proshutinsky, A., Tateyama, K., Williams, W. J., Carmack, E. C., McLaughlin, F. A., & Timmermans, M.-L. (2014). Deterioration of perennial sea ice in the Beaufort Gyre from 2003 to 2012 and its impact on the oceanic freshwater cycle. *Journal of Geophysical Research: Oceans*, *119*, 1271–1305. https://doi.org/10.1002/2013JC008999

Kurtz, N. T., Farrell, S. L., Studinger, M., Galin, N., Harbeck, J. P., Lindsay, R., et al. (2013). Sea ice thickness, freeboard, and snow depth products from Operation IceBridge airborne data. *The Cryosphere*, *7*, 1035–1056. https://doi.org/10.5194/tc-7-1035-2013

Kwok, R., & Rothrock, D. A. (1999). Variability of Fram Strait flux and North Atlantic Oscillation. *Journal of Geophysical Research*, *104*, 5177–5189. https://doi.org/10.1029/1998jc900103

Kwok, R., & Rothrock, D. A. (2009). Decline in Arctic sea ice thickness from submarine and ICESat records: 1958–2008. *Geophysical Research Letters*, *36*, L15501. https://doi.org/10.1029/2009GL039035

Levitus, S. (1982). *Climatological Atlas of the World Ocean (NOAA Proferssional Paper No. 13)* (p. 173). U.S. Govt. Printing Office.

Li, M., Ke, C.-Q., Shen, X., Cheng, B., & Li, H. (2020). Investigation of the Arctic Sea ice volume from 2002 to 2018 using multi-source data. *International Journal of Climatology*, 2509–2527. https://doi.org/10.1002/joc.6972

Lindsay, R. (2013). *Unified Sea Ice Thickness Climate Data Record Collection Spanning 1947-2012*. Boulder, Colorado USA: National Snow and Ice Data Center. https://doi.org/10.7265/N5D50JXV

Lindsay, R., & Schweiger, A. (2015). Arctic sea ice loss determined using subsurface, aircraft, and satellite observations. *Cryosphere*, *9*, 269–283. https://doi.org/10.5194/tc-9-269-2015

Lindsay, R. W. (2010). Unified sea ice thickness climate data record. Polar Science Center, Applied Physics Laboratory, University of Washington.

Maykut, G. A., & Untersteiner, N. (1971). Some results from a time-dependent thermo-dynamic model of sea ice. *Journal of Geophysical Research*, *76*, 1550–1575. https://doi.org/10.1029/jc076i006p01550

Melling, H., & Riedel, D. A. (2008). *Ice Draft and Ice Velocity Data in the Beaufort Sea, 1990–2003*. Boulder, Colorado USA: National Snow and Ice Data Center.

Parkinson, C. L., & Comiso, J. C. (2013). On the 2012 record low Arctic sea ice cover: Combined impact of preconditioning and an August storm. *Geophysical Research Letters*, *40*, 1356–1361. https://doi.org/10.1002/grl.50349

Petty, A. A., Holland, M. M., Bailey, D. A., & Kurtz, N. T. (2018). Warm Arctic, increased winter sea ice growth? *Geophysical Research Letters*, *45*, 12922–12930. https://doi.org/10.1029/2018GL079223

Rampal, P., Weiss, J., & Marsan, D. (2009). Positive trend in the mean speed and deformation rate of Arctic sea ice, 1979–2007. *Journal of Geophysical Research*, *114*. https://doi.org/10.1029/2008JC005066

Richter-Menge J., Overland J. E., & Mathis J. T. (Eds.), (2016). *Arctic report card 2016*. Retrieved from http://www.arctic.noaa.gov/Report-Card

Rothrock, D. A., Percival, D. B., & Wensnahan, M. (2008). The decline in arctic sea-ice thickness: Separating the spatial, annual, and interannual variability in a quarter century of submarine data. *Journal of Geophysical Research*, *113*. https://doi.org/10.1029/2007jc004252

Schweiger, A., Lindsay, R., Zhang, J., Steele, M., Stern, H., & Kwok, R. (2011). Uncertainty in modeled Arctic sea ice volume. *Journal of Geophysical Research*, *116*. https://doi.org/10.1029/2011JC007084

Serreze, M. C., Holland, M. M., & Stroeve, J. (2007). Perspectives on the Arctic's shrinking sea-ice cover. *Science*, *315*, 1533–1536. https://doi.org/10.1126/science.1139426

Smith, R. D., Dukowicz, J. K., & Malone, R. C. (1992). Parallel ocean general circulation modeling. *Physica D*, 38–61.

Spreen, G., Kwok, R., & Menemenlis, D. (2011). Trends in Arctic sea ice drift and role of wind forcing: 1992–2009. *Geophysical Research Letters*, *39*. https://doi.org/10.1029/2011GL048970

Stroeve, J. C., Schroder, D., Tsamados, M., & Feltham, D. (2018). Warm winter, thin ice? *The Cryosphere*, *12*, 1791–1809. https://doi.org/10.5194/tc-12-1791-2018

Stroeve, J., Serreze, M., Drobot, S., Gearheard, S., Holland, M., Maslanik, J., et al. (2008). Arctic sea ice extent plummets in 2007. *Eos, Transactions American Geophysical Union*, *89*(2), 13–14. https://doi.org/10.1029/2008eo020001

Thorndike, A. S., Rothrock, D. A., Maykut, G. A., & Colony, R. (1975). The thickness distribution of sea ice. *Journal of Geophysical Research*, *80*, 4501–4513. https://doi.org/10.1029/jc080i033p04501

Wang, Q., Ricker, R., & Mu, L. (2021). Arctic sea ice decline preconditions events of anomalously low sea ice volume export through Fram Strait in the early 21st century. *Journal of Geophysical Research*, *126*, e2020JC016607. https://doi.org/10.1029/2-2-JC016607

Winton, M. (2000). A reformulated three-layer sea ice model. *Journal of Atmospheric and Oceanic Technology*, *17*, 525–531. https://doi.org/10.1175/1520-0426(2000)017<0525:ARTLSI>2.0.CO;2

Witte, H., & Fahrbach, E. (2005). *AWI Moored ULS Data, Greenland Sea and Fram Strait, 1991-2002 edited*. National Snow and Ice Data Center.

Zhang, J., Ashjian, C., Campbell, R., Spitz, Y. H., Steele, M., & Hill, V. (2015). The influence of sea ice and snow cover and nutrient availability on the formation of massive under-ice phytoplankton blooms in the Chukchi Sea. *Deep Sea Research Part II: Topical Studies in Oceanography*, *118*, 122–135. https://doi.org/10.1016/j.dsr2.2015.02.008

Zhang, J., & Hibler, W. D. (1997). On an efficient numerical method for modeling sea ice dynamics. *Journal of Geophysical Research*, *102*, 8691–8702. https://doi.org/10.1029/96jc03744

Zhang, J., Lindsay, R., Schweiger, A., & Rigor, I. (2012). Recent changes in the dynamic properties of declining Arctic sea ice: A model study. *Geophysical Research Letters*, *39*, L20503. https://doi.org/10.1029/2012GL053545

Zhang, J., Lindsay, R. W., Steele, M., & Schweiger, A. (2008). What drove the dramatic retreat of Arctic sea ice during summer 2007? *Geophysical Research Letters*, *35*. https://doi.org/10.1029/2008GL034005

Zhang, J., & Rothrock, D. A. (2003). Modeling global sea ice with a thickness and enthalpy distribution model in generalized curvilinear coordinates. *Monthly Weather Review*, *131*(5), 681–697. https://doi.org/10.1175/1520-0493(2003)131<0845:MGSIWA>2.0.CO;2

Zhang, J., & Rothrock, D. A. (2005). The effect of sea-ice rheology in numerical investigations of climate. *Journal of Geophysical Research*, *110*. https://doi.org/10.1029/2004JC002599